Co-registered Cardiac *ex vivo* DT Images and Histological Images for Fibrosis Quantification

Peter Lin[1,2], Anne Martel[1,2], Susan Camilleri[3], and Mihaela Pop[1,2(✉)]

[1] Sunnybrook Research Institute, Toronto, Canada
mihaela.pop@utoronto.ca
[2] Medical Biophysics, University of Toronto, Toronto, Canada
[3] Lunenfeld Research Institute, Toronto, Canada

Abstract. Cardiac magnetic resonance (MR) imaging can detect infarct scar, a major cause of lethal arrhythmia and heart failure. Here, we describe a robust image processing pipeline developed to quantitatively analyze collagen density and features in a pig model of chronic fibrosis. Specifically, we use *ex vivo* diffusion tensor imaging (DTI) ($0.6 \times 0.6 \times 1.2$ mm resolution) to calculate fractional anisotropy maps in: healthy tissue, infarct core (IC) and gray zone (GZ) (i.e., a mixture of viable myocytes and collagen fibrils bordering IC and healthy zones). The 3 zones were validated using collagen-sensitive histological slides co-registered with MR images. Our results showed a significant ($p < 0.05$) reduction in the mean FA values of GZ (by 17%) and IC (by 44%) compared to healthy areas; however, we found that these differences do not depend on the location of occluded coronary artery (LAD vs LCX). This work validates the utility of DTI-MR imaging for fibrosis quantification, with histological validation.

Keywords: Myocardial infarct · DTI · Fibrosis · Image registration

1 Introduction

Ventricular arrhythmia and progressive heart failure associated with structural disease (e.g. chronic infarction) are major causes of death worldwide. In the clinics, the location of the fibrotic infarct is evaluated non-invasively using MR imaging [1]. In these MR images, heterogeneous fibrosis has an intermediate signal intensity between healthy (H) tissue and infarct core (IC), and is therefore named 'gray zone' (GZ) [9]. However, the clinical spatial MR resolution is often inadequate (i.e., 8–10 mm slice thickness) resulting in an overestimated GZ and IC extent due to partial volume effects [6,7]. Furthermore, in post-infarction patients, subtle fibrosis characteristics (e.g. alteration in myocardial tissue anisotropy) cannot be properly detected due to motion-related MR artifacts nor they can be histologically validated.

Fractional anisotropy (FA) is a scalar metric calculated from DTI-derived eigenvectors that describes the degree of diffusivity of water molecules in tissue. Regions with replacement fibrosis have lower FA due to increased myocardial fiber disarray resulting from local necrosis, ventricular remodeling, and infiltration of thin collagen fibrils, thus increasing the diffusivity of water molecules [8,13].

Our broad aim is to use high-resolution MR to identify subtle characteristics of heterogeneous fibrosis in a pre-clinical model of chronic infarction with histological validation, and construct 3D MRI-based models for simulations [3,10]. This type of fibrosis harbors the foci of lethal arrhythmia and is comprised of a mixture of healthy myocytes and collagen fibrils, bordering dense scar areas [4]. In this work, we aim to develop an image analysis pipeline to study myocardial anisotropy in GZ by means of high-resolution diffusion-weighted MR images acquired in explanted pig hearts. Specifically, we use DTI to calculate FA (as a measure of fiber disarray in GZ/IC), and correlate these FA maps with collagen density from co-registered histological images using affine registration.

2   Materials and Methods

2.1   Animal Model of Myocardial Infarction

Myocardial infarction was generated in Yorkshire swines (N = 10) using a 90-min occlusion-reperfusion method under x-ray fluoroscopy, as previously described in [8]. The infarctions were induced in the LAD territory of 5 pigs, and in the LCX territory of another 5 pigs. They were then allowed to heal for 5–6 weeks prior to animal sacrifice, heart explantation, and MR imaging. All animal experiments received ethical approval from Sunnybrook Research Institute, Toronto and were conducted in accordance with protocols instated by the Animal Care Committee of Sunnybrook Health Sciences Centre, Toronto.

2.2   *Ex Vivo* Diffusion-Weighted MR Imaging

All diffusion-weighted MR images were acquired using a 1.5T GE Sigma Excite scanner. The explanted hearts were fixed in 10% formalin for 3–4 days and then placed in a Plexiglas phantom box filled with Fluorinert (3M^{TM}, USA) for imaging. Each heart phantom was placed in an eight-channel head coil. The following MR parameters for diffusion-weighted imaging were used: echo time = 35 ms, repetition time = 700 ms, FOV = 160×160 mm, slice thickness = 1.2 mm, matrix = 256×256, b value = 0 s/mm^2 for unweighted images, and b = 500 s/mm^2 for diffusion-weighted images in 7 diffusion sampling gradients. The in-plane image resolution was $0.6 \times 0.6 \times 1.2$ mm and the total scan time for each heart was approximately 10 h.

2.3   Fractional Anisotropy Map Calculation

The equations describing DT imaging and eigenanalysis are described below [2]. The DWI echo signal intensity S is calculated by the following:

$$S = S_0 e^{-b \cdot D} \tag{1}$$

where S^0 is the signal of the unweighted image ($b = 0$). The b value is a diffusion weighing factor that describes the strength and timing of diffusion gradients, which is used to compute the diffusion-weighted image. D is a diffusion coefficient of water molecules and can be represented by a 3×3 tensor as shown in Eq. 2:

$$D = \begin{bmatrix} D_{xx} & D_{xy} & D_{xz} \\ D_{yx} & D_{yy} & D_{yz} \\ D_{zx} & D_{zy} & D_{zz} \end{bmatrix} = E^T \begin{bmatrix} \lambda_1 & 0 & 0 \\ 0 & \lambda_2 & 0 \\ 0 & 0 & \lambda_3 \end{bmatrix} E \tag{2}$$

This tensor is derived from directional diffusivities and is symmetric such that $D_{ij} = D_{ji}$, with $i, j = x, y, z$. Thus, there are only six independent variables in this tensor. E represents a matrix of three eigenvectors, indicating the direction of the principle axes of the tensor model. λ_1, λ_2 and λ_3 represent eigenvalues describing the size of principle axes.

Equation 3 shows the formula for FA for each voxel. For a perfect isotropic medium, $\lambda_1 = \lambda_2 = \lambda_3$ and $FA = 0$, whereas with progressive diffusion anisotropy, $FA \rightarrow 1$ (e.g. healthy myocardial muscle fibers).

$$FA = \frac{\sqrt{3}}{\sqrt{2}} \frac{\sqrt{(\lambda_1 - \lambda)^2 + (\lambda_2 - \lambda)^2 + (\lambda_3 - \lambda)^2}}{\sqrt{\lambda_1^2 + \lambda_2^2 + \lambda_3^2}} \tag{3}$$

2.4   Histopathology

From each heart, one representative 4 mm thick slab was cut in short-axis orientation (matching one DT image), sectioned to focus on the infarcted region, and then paraffin embedded. Thin slices were cut from these slabs at 4 μm thickness using a microtome, mounted on small 1×3 inch glass slides and stained. To visualize collagenous fibrosis, the slides were stained with picrosirius red and scanned at 40× magnification using a TISSUEscope TM 4000 confocal microscope (Huron Technologies International Inc.).

2.5   Fibrosis Quantification

In this work, we aimed to quantify fibrosis in FA maps (calculated from DTI) for each myocardial zone defined by the collagen density in histological images: H, GZ and IC. The pipeline for this process is briefly outlined in Fig. 1.

For each heart, FA maps were reviewed to manually select the slice corresponding to the histology image. Histology images and FA maps were then overlaid in the open source software Sedeen Viewer (Pathcore 2018)[1] for manual registration using anatomical landmarks (e.g., papillary muscles, scar morphology).

---

[1] https://pathcore.com/sedeen/.
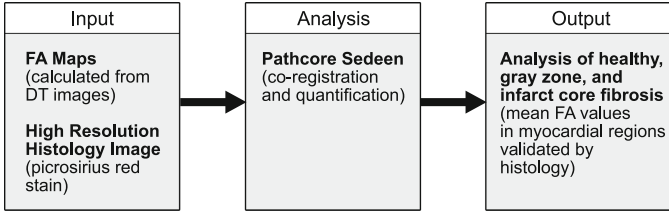
Fig. 1. Illustration of the image processing pipeline. FA maps were manually registered with histology images for collagen quantification. H, GZ and IC regions were validated with ground truth histology.

Affine registration was performed to correct non-uniform tissue shrinkage effects from tissue fixation and histology processing. This approach is more appropriate than rigid registration because it allows image scaling. Once registered, 3×3 MR pixel regions of interest (ROI) were selected on the histology image for stain quantification. For each heart, 2 ROIs were selected from each of H, GZ and IC zones. The stain analysis plugin [5] in Sedeen was used to quantify tissues with a positive stain for collagen and return a percent collagen composition for each ROI. Using our previous grading system, this plugin was used to classify each tissue category as either H ($<20\%$ collagen), GZ (20–70% collagen) or IC ($>70\%$ collagen) [8]. Once classified, the same ROI was imposed onto a FA map for mean FA calculations using DSI Studio (Labsolver 2018)[2].

2.6   Statistical Analysis

Mean FA values were expressed as mean ± 1 SD. Tukey boxplots were used to compare mean FA values in each of the 3 cardiac zones (H, GZ and IC). Student's t-tests were performed to evaluate levels of significance between groups ($p < 0.05$). One-way analysis of variance (ANOVA) was performed to determine statistically significant differences in mean FA values in H, GZ and IC regions. All statistical tests were performed using RStudio Version 1.1.463 (RStudio Inc. 2018).

3   Results

Figure 2 shows the steps of quantitatively analyzing FA values in one heart. The bottom-right image illustrates an analyzed ROI showing pixels with a positive stain for collagen (red). The bottom-left image shows the corresponding ROI on the FA map, which is a gray-scale display of FA values across the image with brighter areas being more anisotropic than darker areas (i.e., IC).

Figure 3 shows the resulting mean FA for the 3 zones: H (0.52 ± 0.12), GZ (0.43 ± 0.13) and IC (0.29 ± 0.17). We observed a significant difference in FA

---

[2] http://dsi-studio.labsolver.org.
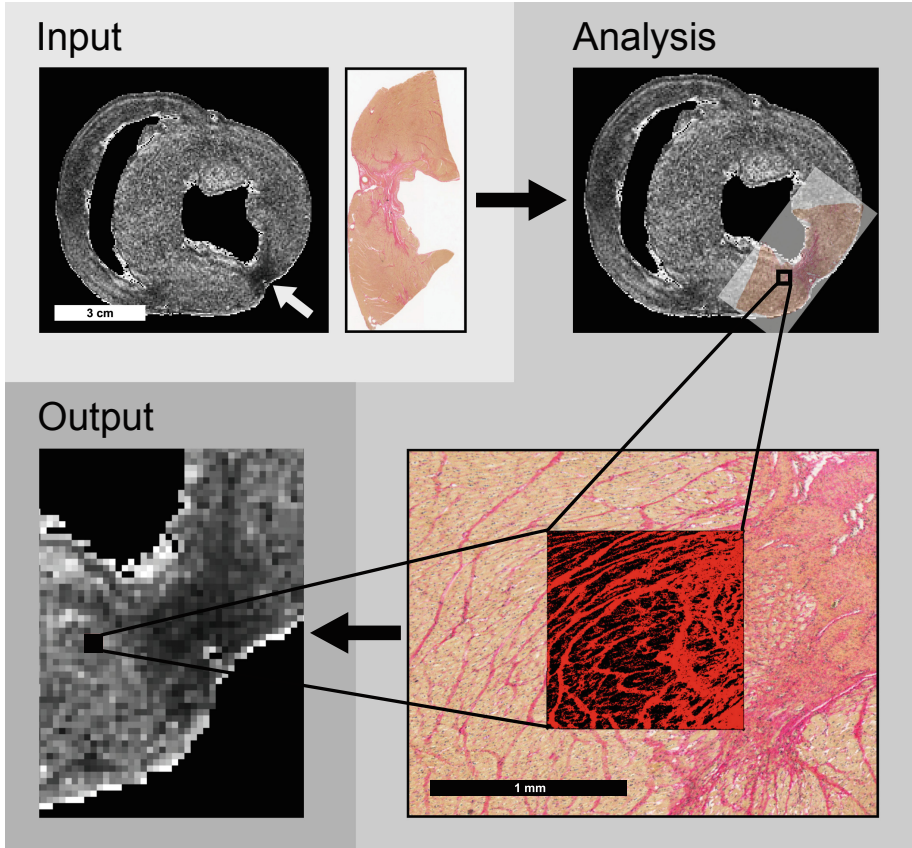
Fig. 2. Example of a co-registered histology image and FA map for quantitative collagen analysis, where the white arrow points to the infarct generated in the LCX territory. The magnified ROI in the bottom right figure shows an example of GZ classification (34% collagen) using the stain analysis plugin in Sedeen. Once the histology-based ROI was classified, a mean FA value (0.38) for its corresponding ROI in the FA map was calculated as shown in the bottom-left figure. (Color figure online)

values between all 3 zones (one way $ANOVA = 1.8 \times 10^{-5}$). Figure 4 shows the comparison of FA values between the LAD and LCX sub-groups for each region. Notably, we found no statistical difference between these 2 groups.

Figure 5 illustrates an exemplary snapshot taken from the visualization and analysis software Sedeen, in which we co-registered the FA map and the picrosirius red image at 50% opacity. Here, 2 ROIs selected from each of: H, GZ and IC regions are visible on the registered image (yellow squares).
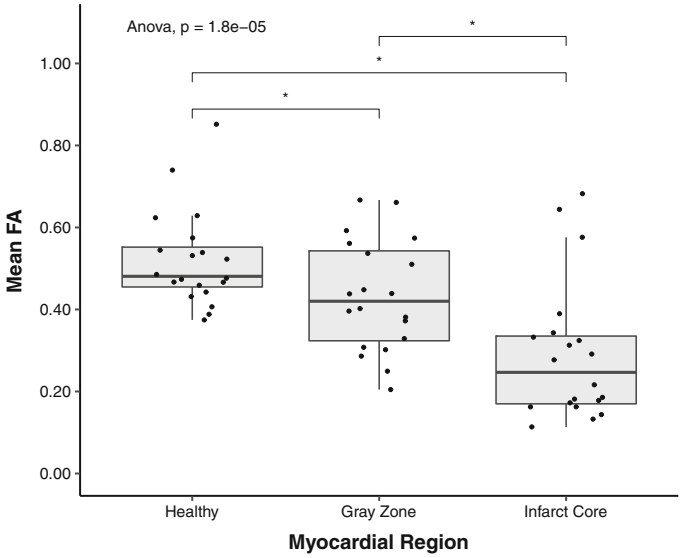
Fig. 3. Results from FA analysis. Mean FA values in healthy, gray zone and infarct core myocardium illustrated using a Tukey boxplot. Lines in the boxplots represent the statistical median. Error bars reflect the lowest and highest data point within 1.5 interquartile range of the lower and upper quartiles respectively. (* $=$ p < 0.05 in an independent samples t-test).
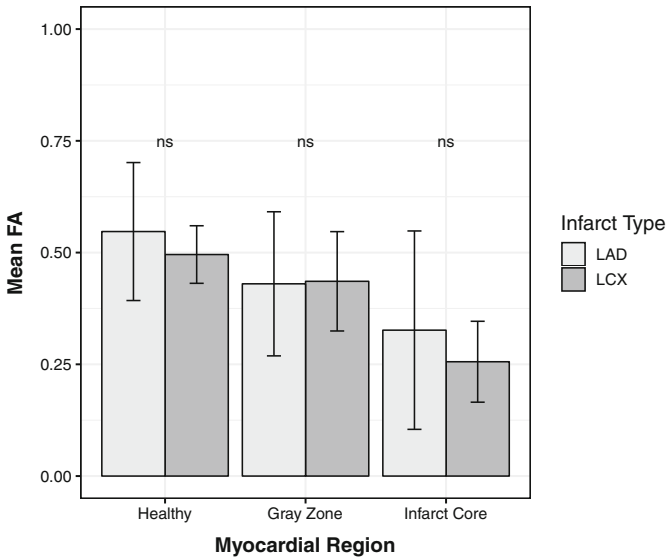
Fig. 4. Results from FA analysis. Bar graph displaying FA values in each cardiac region stratified by infarct type. Error bars reflect ± 1 SD. (ns $=$ not significant in an independent samples t-test).
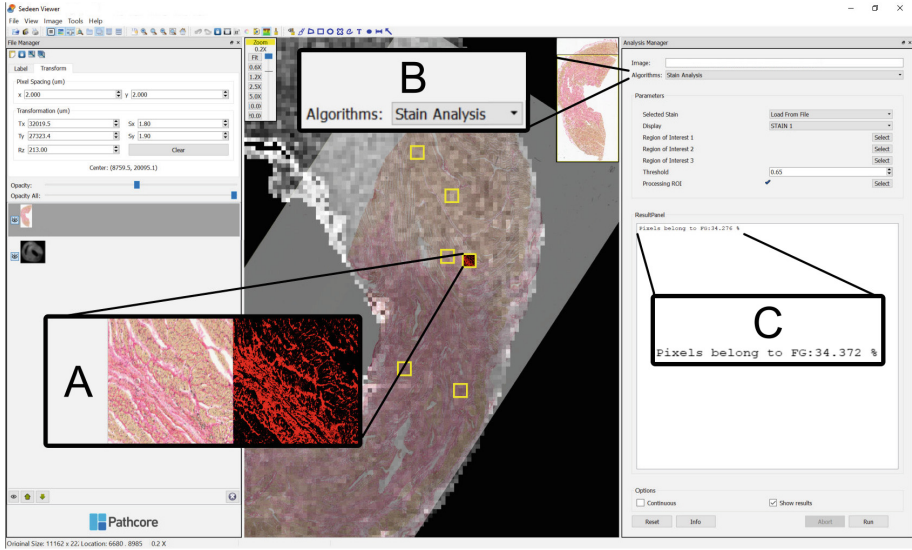
Fig. 5. Visualization of the Sedeen user interface, including its native file manager (left menu) and analysis manager (right menu). (A) shows a magnified image of one analyzed ROI. The left image is acquired from the raw histology image and the right image is the same region following analysis of the collagen stain. (B) shows the user-interface for algorithm selection. For stain quantification, we used the stain analysis plugin. (C) is a magnified image of showing the output of the stain analysis plugin. Here, we can quantitatively assess the percent collagen composition of this ROI and thus classify it as one of: H, GZ or IC. (Color figure online)

4 Discussion and Conclusion

In this work, we describe an image processing pipeline focused on co-registered histology and MR images to quantitatively assess the extent of collagenous fibrosis in H, GZ and IC myocardium using FA, a measure of the diffusivity of water molecules reflecting tissue architecture and alignment.

In histologically-classified ROIs, we found that mean FA decreases significantly in GZ (reduction of 17%, from $0.52 \pm 0.12 \rightarrow 0.43 \pm 0.13$, $p = 0.034$) and IC (reduction of 44%, from $0.52 \pm 0.12 \rightarrow 0.29 \pm 0.17$, $p = 0.00005$) myocardial zones when compared to healthy tissue. Our results are consistent with findings from Wu et al. [17], who investigated FA in porcine hearts with myocardial infarction and observed a decrease in the IC (38.4%) and GZ (6.1%). Unlike our study which performed mean FA calculations on small histologically-classified ROIs, they performed calculations on 8 large radial segments of the left ventricle which may represent a confounding mixture of both healthy and scar tissue. These FA values, in addition to the patterns of FA reduction, are similar to studies using human models of myocardial infarction, further validating our porcine model for studying myocardial infarction as seen in the clinic [14,15].

This decrease in FA is likely multifactorial, involving the loss of healthy myocyte architecture and the deposition of replacement fibrosis. Healthy myocardium is known to be highly anisotropic, reflecting its directionally organized fibers and conductive properties; however, following myocardial infarction, networks of functional myocytes are replaced by collagenous fibrosis [11,12].

Notably, we report no differences in FA between LAD and LCX sub-groups, suggesting that tissue anisotropy in H, GZ, and IC myocardial zones may not depend on infarct location. This finding is also consistent with Wu et al. [16] who compared non-reperfused occlusion-induced LAD and LCX infarctions in pig. Comparable results between two different models of infarction (our occlusion-reperfusion model vs the non-reperfusion occlusion model in [16]) indicates that patterns of tissue fibrosis, as characterized by FA measurements, are also largely independent of infarct location.

Lastly, we acknowledge limitations in our method. For the calculation of diffusion tensor, our fitting model used only 2 b-values (0 and 500) rather than 3. Our *ex vivo* high-resolution image acquisition time was roughly 10 h; thus, it was unfeasible to perform another scan for the additional fitting. Additionally, we registered *ex vivo* MR images with heart tissue using affine registration for scaling. This approach is acceptable for our work since all images (diffusion-weighted and histology) were acquired *ex vivo* following fixation; however, further investigations using *in vivo* MR images are warranted to better reflect tissue anisotropy under physiological conditions. These MR images would be subject to motion-related artifacts and differences in morphology due to *in vivo* conditions. As such, deformable image registration techniques using anisotropy scale factors may be necessary in addition to metrics for registration confidence. Notably, Sedeen can perform manual anisotropic transformations with the potential for semi-automatic registration plugins. As such, this image processing pipeline may be applied to *in vivo* studies in the future.

To conclude, this study describes a robust image processing pipeline for anisotropy characterization in myocardial infarction using high resolution DTI and histologically-classified ROIs in a chronic fibrotic scar. In doing so, we find that FA, a measure of tissue fibrosis, decreases significantly from H to GZ to IC myocardial zones. We also report that the degree of collagenous fibrosis as quantified by FA is largely independent of infarct territory (LAD or LCX). Overall, we demonstrate that DTI as a non-invasive imaging modality can identify subtle differences between H, GZ and IC tissue.

References

1. Bello, D., et al.: Infarct morphology identifies patients with substrate for sustained ventricular tachycardia. J. Am. Coll. Cardiol. **45**(7), 1104–1108 (2005)

2. Jiang, H., van Zijl, P.C., Kim, J., Pearlson, G.D., Mori, S.: DtiStudio: resource program for diffusion tensor computation and fiber bundle tracking. Comput. Methods Programs Biomed. **81**(2), 106–116 (2006)

3. Li, M., et al.: Pipeline to build and test robust 3D T1 mapping-based heart models for EP interventions: preliminary results. In: Coudière, Y., Ozenne, V., Vigmond, E., Zemzemi, N. (eds.) FIMH 2019. LNCS, vol. 11504, pp. 64–72. Springer, Cham (2019). https://doi.org/10.1007/978-3-030-21949-9_8

4. Lin, P., et al.: High resolution imaging and histopathological characterization of myocardial infarction. Biophys. J. **116**(3), 231a (2019)

5. Martel, A.L., et al.: An image analysis resource for cancer research: PIIP— Pathology Image Informatics Platform for visualization, analysis, and management. Cancer Res. **77**(21), e83–e86 (2017)

6. Mekkaoui, C., Reese, T.G., Jackowski, M.P., Bhat, H., Sosnovik, D.E.: Diffusion MRI in the heart. NMR Biomed. **30**(3), e3426 (2017)

7. Nguyen, C., et al.: In vivo three-dimensional high resolution cardiac diffusion-weighted MRI: a motion compensated diffusion-prepared balanced steady-state free precession approach: 3D high resolution cardiac DW-MRI via diffusion-prepared bSSFP. Magn. Reson. Med. **72**(5), 1257–1267 (2014)

8. Pop, M., et al.: Quantification of fibrosis in infarcted swine hearts by ex vivo late gadolinium-enhancement and diffusion-weighted MRI methods. Phys. Med. Biol. **58**(15), 5009–5028 (2013)

9. Pop, M., et al.: High-resolution 3-D T1*-mapping and quantitative image analysis of GRAY ZONE in chronic fibrosis. IEEE Trans. Biomed. Eng. **61**(12), 2930–2938 (2014)

10. Pop, M., et al.: Construction of 3D MR image-based computer models of pathologic hearts, augmented with histology and optical fluorescence imaging to characterize action potential propagation. Med. Image Anal. **16**(2), 505–523 (2012)

11. Prabhu, S.D., Frangogiannis, N.G.: The biological basis for cardiac repair after myocardial infarction: from inflammation to fibrosis. Circ. Res. **119**(1), 91–112 (2016)

12. Valderrabano, M.: Influence of anisotropic conduction properties in the propagation of the cardiac action potential. Prog. Biophys. Mol. Biol. **94**(1–2), 144–168 (2007)

13. Whittaker, P., Boughner, D.R., Kloner, R.A.: Analysis of healing after myocardial infarction using polarized light microscopy. Am. J. Pathol. **134**(4), 15 (1989)

14. Winklhofer, S., et al.: Post-mortem cardiac diffusion tensor imaging: detection of myocardial infarction and remodeling of myofiber architecture. Eur. Radiol. **24**(11), 2810–2818 (2014)

15. Wu, E.X., et al.: MR diffusion tensor imaging study of postinfarct myocardium structural remodeling in a porcine model. Magn. Reson. Med. **58**(4), 687–695 (2007)

16. Wu, Y., Chan, C.W., Nicholls, J.M., Liao, S., Tse, H.F., Wu, E.X.: MR study of the effect of infarct size and location on left ventricular functional and microstructural alterations in porcine models. J. Magn. Reson. Imaging **29**(2), 305–312 (2009)

17. Wu, Y., Tse, H.F., Wu, E.X.: Diffusion tensor MRI study of myocardium structural remodeling after infarction in porcine model. In: 2006 International Conference of the IEEE Engineering in Medicine and Biology Society, pp. 1069–1072. IEEE (2006)